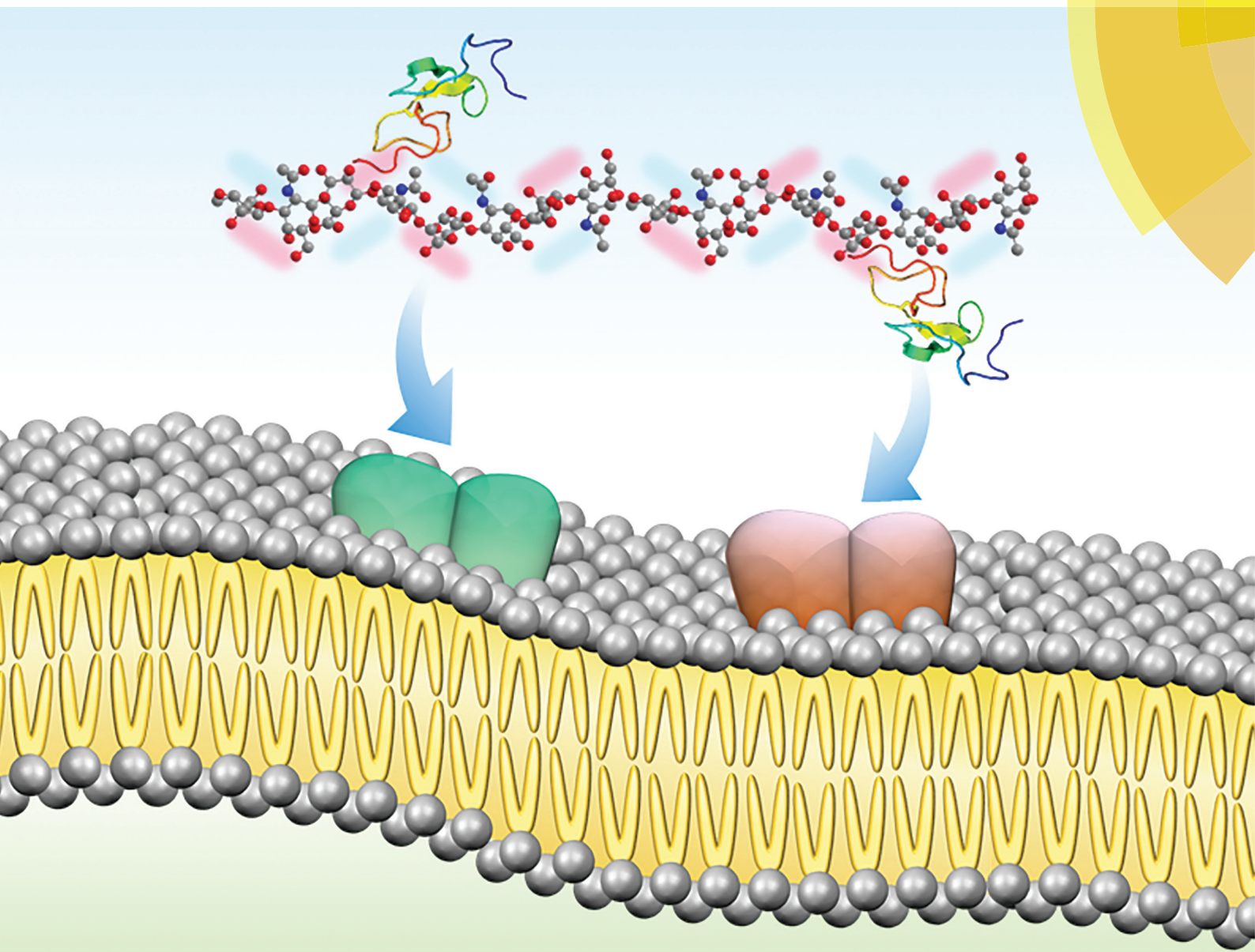


Biomaterials Science

rsc.li/biomaterials-science



ISSN 2047-4849



PAPER


Sei Kwang Hahn *et al.*
Synergistic effects of hyaluronate – epidermal growth factor conjugate patch on chronic wound healing





Cite this: *Biomater. Sci.*, 2018, **6**, 1020

Synergistic effects of hyaluronate – epidermal growth factor conjugate patch on chronic wound healing

Yun Seop Kim,^a Dong Kyung Sung,^b Won Ho Kong,^a Hyemin Kim^a and Sei Kwang Hahn *^a

The proteolytic microenvironment in the wound area reduces the stability and the half-life of growth factors *in vivo*, making difficult the topical delivery of growth factors. Here, epidermal growth factor (EGF) was conjugated to hyaluronate (HA) to improve the long-term stability against enzymatic degradation and the therapeutic effect by enhancing the biological interaction with HA receptors on skin cells. After the synthesis of HA–EGF conjugates, they were incorporated into a patch-type formulation for the facile topical application and sustained release of EGF. According to ELISA, the HA–EGF conjugates showed a long-term stability compared with native EGF. Furthermore, HA–EGF conjugates appeared to interact with skin cells through two types of HA and EGF receptors, resulting in a synergistically improved healing effect. Taken together, we could confirm the feasibility of HA–EGF conjugates for the transdermal treatment of chronic wounds.

Received 22nd January 2018,
Accepted 11th March 2018

DOI: 10.1039/c8bm00079d

rsc.li/biomaterials-science

Introduction

Chronic wounds such as diabetic ulcers arise from tissue injuries that heal slowly. Unlike acute wounds, the exudate from chronic wounds contains relatively high levels of tissue-destructive proteases and low levels of growth factors, resulting in poor wound healing.^{1,2} The application of exogenous growth factors may compensate for the lack of endogenous growth stimulation. Growth factors influence and modulate epidermal and dermal regeneration, angiogenesis, and granulation formation, but all these processes are inhibited in chronic wounds. The native growth factors are short-lived in the highly proteolytic wound environment, requiring repeated topical applications. The use of native growth factors makes wound healing therapies expensive due to a large amount of dose with questionable efficacy in the proteolytic wound environment of the skin.

The covalent conjugation of poly(ethylene glycol) (PEG) to proteins (PEGylation) has become a popular method to increase stability, decrease immunogenicity and antigenicity, and increase the half-life of proteins *in vivo*. Other polymers

for the protein conjugation have been developed with the aim of improving the biological function and providing a better stability.^{3,4} For example, Keefe *et al.* demonstrated that the covalent conjugation of poly(carboxybetaine) to α -chymotrypsin improved the enzyme stability retaining its native binding affinity.⁵ A dextrin–recombinant human epidermal growth factor (rhEGF) conjugate was synthesized for masking rhEGF bioactivity and preventing the proteolysis by neutrophil elastase.^{6–8} The conjugation of growth factors to heparin can also extend their half-lives and enhance their binding affinity to cell surface receptors for intracellular signaling, thereby increasing the bioactivity.^{9,10} Furthermore, another research group developed a heparin-mimicking polymer that stabilizes fibroblast growth factors and activates fibroblast growth factor receptors.^{11–13} We previously reported the conjugation of hyaluronate (HA) with human growth hormones (hGH) for effective transdermal delivery.¹⁴

Among various biomacromolecules, HA is well known for remarkable characteristics such as hygroscopic, rheological, biocompatible, immunocompatible, and viscoelastic properties. In addition, HA facilitates regeneration and wound healing by regulating cell functions *via* binding to receptors such as cluster determinant 44 (CD44) and receptor for HA mediated motility (RHAMM) expressed on the surface of skin cells including fibroblasts and keratinocytes.¹⁵ In addition, epidermal growth factor (EGF), a single polypeptide chain of 53 amino acids with three interchain disulfide bonds, plays an important role in wound healing owing to its positive effect on

^aDepartment of Materials Science and Engineering, Pohang University of Science and Technology (POSTECH), 77 Cheongamro, Nam-gu, Pohang, Gyeongbuk 37673, Republic of Korea. E-mail: skhanb@postech.ac.kr; Fax: +82 54 279 2399; Tel: +82 54 279 2159

^bDepartment of Pediatrics, Samsung Medical Center, School of Medicine, Sungkyunkwan University, 81 Irwon-ro, Gangnam-gu, Seoul 06351, Republic of Korea

collagen deposition and proliferation, and migration of keratinocytes, fibroblasts and vascular endothelial cells at the wound area.¹⁶

In this work, we developed HA-EGF conjugates to protect from proteolytic degradation by trypsin and improve the biological interaction with skin cells of keratinocytes for facilitated chronic wound healing. The synthesized HA-EGF conjugate was characterized by gel permeation chromatography (GPC), circular dichroism (CD) spectroscopy, enzyme-linked immunosorbent assay (ELISA), and Bradford assay. The synergistic effect of HA-EGF conjugates on keratinocytes was assessed by confocal microscopy, flow cytometric analysis, proliferation assay, and ELISA. After that, we incorporated the conjugates into highly concentrated HA patches for long-term sustained release of the conjugates *in vivo*. The prepared patch-type HA-EGF conjugates were applied for the long-term retention of EGF on the wound area and thereby improved the therapeutic effect in diabetic wound model rats.

Experimental

Materials

Sodium hyaluronate (HA) was purchased from Lifecore Biomedical (Chaska, MN). Recombinant human EGF was obtained from Genscript (Piscataway, NJ). Sodium periodate, sodium cyanoborohydride, ethyl carbazate, *tert*-butyl carbazate, trypsin, streptozotocin (STZ), and fluorescein isothiocyanate isomer I (FITC) were obtained from Sigma-Aldrich (St Louis, MO). An Illustra NAP-5 column was purchased from GE Healthcare (Buckinghamshire, UK) and phosphate buffered saline (PBS, pH 7.4) from Tech & Innovation (Seoul, Korea). The Coomassie Plus (Bradford) protein assay reagent was purchased from Thermo Scientific (Rockford, IL) and the human EGF ELISA kit was obtained from Peprotech (Rocky Hill, NJ). The hydroxyproline assay kit was purchased from Abcam, Inc. (Cambridge, MA) and 3-(4,5-dimethylthiazol-2-yl)-2,5-diphenyl-tetrazolium bromide (MTT) was purchased from Promega (Madison, WI). A 24-well transwell insert was purchased from Millipore (Bedford, MA). Polydimethylsiloxane (PDMS, Sylgard 184) was purchased from Hana Technology (Anyang, Korea). Immortalized human epidermal keratinocytes (HaCaT cells) were kindly donated by Kyong-Tai Kim (POSTECH, Pohang, Korea). Dulbecco's modified Eagle's medium (DMEM) was purchased from Gibco (Grand Island, NY). Human vascular endothelial growth factor (VEGF), rat tumor necrosis factor- α (TNF- α) and interleukin-1 (IL-1) ELISA kits were purchased from eBioscience (Vienna, Austria). The transforming growth factor- β (TGF- β) ELISA kit was purchased from R&D Systems (Minneapolis, MN). All chemicals were used without further purification. Male SD rats weighing 230–250 g were purchased from Orient (Seoul, Korea). All the procedures and experimental protocols were reviewed and approved by the Institutional Animal Care and Use Committee (IACUC) of Samsung Biomedical Research Institute (SBRI).

Synthesis of HA-EGF conjugates

Aldehyde-modified HA (HA-ALD) was prepared to synthesize HA-EGF conjugates. Briefly, 0.5 g of HA with a molecular weight (MW) of 200 kDa was dissolved in 50 mL of distilled water. Two molar excess of sodium periodate was added to the HA solution and stirred for 6 h in the dark. Ethylene glycol (0.5 mL) was added to the reaction mixture and stirred for 2 h to terminate the reaction. The resulting product was poured into a dialysis membrane tube (MW cut off = 10 kDa) and dialyzed against 0.1 M of NaCl aqueous solution and distilled water for 3 days. The aldehyde content was analyzed by ¹H NMR (DPX500, Bruker, Germany). After that, 1 mg of EGF dissolved in PBS (pH 7.4) was transferred to sodium acetate buffer (pH 5.5) using Illustra NAP-5 columns and mixed with HA-ALD having an aldehyde content of 20 mol%. The HA-EGF conjugate was synthesized by the coupling reaction between aldehyde groups of HA-ALD and N-terminal amine groups of EGF. The number of EGF molecules per single HA chain in the feed was adjusted to be 10. Sodium cyanoborohydride at 5 molar excess of HA repeating unit was added for the reduction of hydrazine bonds at room temperature for 24 h. After conjugation, 5 molar excess of ethyl carbazate was added with sodium cyanoborohydride and stirred for 24 h to block the remaining aldehyde group in HA-EGF conjugates. The resulting HA-EGF conjugate solution was purified using a centrifugal filter (MW cut off = 10 kDa) to remove unreacted EGF and other chemicals. Other HA-EGF conjugates were also synthesized using HA-ALD with a MW of 10 or 100 kDa *via* the same method.

Characterization of HA-EGF conjugates

The synthesized HA-EGF conjugates were analyzed by GPC comparing the retention time before and after the conjugation of HA with EGF. GPC was performed using the following systems: a Waters 717 Plus autosampler, Waters 1525 binary HPLC pump, Waters 2487 dual λ absorbance detector, and Ultrahydrogel™ 1000 connected with an Ultrahydrogel™ 500 column. The mobile phase was PBS at pH 7.4 and the flow rate was 0.4 mL min⁻¹. The detection wavelength was 280 nm. The concentration of EGF in HA-EGF conjugates was determined by using the Bradford assay. The immunological binding affinity of EGF and HA-EGF conjugates to the anti-EGF antibody was assessed by human EGF ELISA. The secondary structure of HA-EGF conjugates was analyzed by CD spectroscopy. The CD spectra of EGF and HA-EGF conjugates in PBS were obtained using a UV spectrophotometer (JASCO J-1500, Essex, UK) under a nitrogen atmosphere. A quartz cuvette with a path length of 2 mm was used and data were acquired at 0.2 mm of intervals with a response time of 1 s. The spectrum of PBS was subtracted from each spectrum and the residual ellipticity was calculated by averaging the results of three scans.

Enzymatic degradation of HA-EGF conjugates

HA-EGF conjugates and EGF (both 1 μ g mL⁻¹) were dissolved in PBS, respectively. To assess protein stability against proteo-

lytic degradation, trypsin was added to the samples and incubated at 37 °C for designated times. Samples (200 μ L) were taken at predetermined times and snap-frozen in liquid nitrogen. At the end of the experiment, all samples were defrosted and analyzed by human EGF ELISA.

***In vitro* stability test of HA-EGF conjugates**

The long-term stability of EGF and HA-EGF conjugate was evaluated by ELISA after incubation in PBS at a concentration of 0.1 mg mL⁻¹ and 37 °C for up to 6 months. At predetermined time intervals, each sample was immediately diluted 5000 times with PBS and stored at -80 °C before ELISA. Samples were analyzed by human EGF ELISA kits. Four replicates were performed for the experiment.

Preparation of patch-type HA-EGF conjugates

The patch-type HA-EGF conjugates were prepared from PDMS molds with 8 mm holes by casting HA solution containing HA-EGF conjugates. PDMS molds were prepared by curing a mixture of PDMS precursors and curing agents (weight ratio of 10:1) at 60 °C for 12 h, followed by punching the cured PDMS sheet with an 8 mm biopsy punch. Before casting HA patches, the molds were sterilized by UV irradiation in the clean bench. HA solution (7 w/v%, 0.2 mL) with a MW of 200 kDa in PBS (pH 7.4) containing EGF (1 μ g) or HA-EGF conjugates (10 μ g, EGF 1 μ g) was poured into the holes of PDMS molds and then dried at 25 °C for 36 h. The prepared HA patches (8 mm disk of 0.5 mm thickness) were sealed and stored at 4 °C prior to use.

Characterization of patch-type HA-EGF conjugates

High resolution field-emission scanning electron microscopy (SEM, JEOL JSM-7410F) was used to characterize the morphology of patch-type HA-EGF conjugates after coating with platinum. To observe the surface of patch-type HA-EGF conjugates with 10, 100, or 200 kDa MW before and after hydration, three types of patch-type HA-EGF conjugates were hydrated for the same time and simultaneously put into liquid nitrogen. A layer of conductive adhesive was pasted to the dedicated SEM object stage and the patches were attached to the stage for the observation of the surface.

FITC labeling of EGF and HA-EGF conjugates

For *in vitro* release and cell-binding tests, EGF and HA-EGF conjugates were fluorescently labeled with FITC. Twenty molar excess of FITC was added to EGF and HA-EGF conjugate solutions dissolved in sodium carbonate buffer (pH 9.0). The reaction mixture was stirred at room temperature overnight in the dark and purified using an Illustra NAP-5 column. The resulting FITC-labeled EGF (EGF-FITC) or FITC-labeled HA-EGF (HA-EGF-FITC) conjugate solution was incorporated into HA patches for further experiments.

***In vitro* release test of HA-EGF conjugates from HA patches**

In vitro release profiles of HA-EGF conjugates incorporated into HA patches were investigated by using transwell inserts.

HA patches containing HA-EGF-FITC conjugates were put onto the upper wells. Then, the lower wells were filled with PBS (pH 7.4) and maintained at 37 °C. At predetermined time points, PBS was sampled from the lower wells, which were refilled with fresh PBS. The amount of the released HA-EGF-FITC conjugate was analyzed by measuring the intensity of FITC fluorescence (Fluoroskan Ascent FL, Thermo LabSystem, Beverly, MA).

Binding test of HA-EGF conjugates to HaCaT cells

HaCaT cells were seeded into the cell culture plate. After incubation for 24 h, excess EGF or HA was added to the cell culture plate for preincubation. Then, the cells were washed with PBS three times and treated with HA-EGF-FITC conjugates. After incubation for 2 h, the cells were washed with PBS three times and analyzed with a confocal microscope (Fluoview FV500, Olympus, Tokyo), flow cytometer (FACSCalibur, BD Biosciences, San Jose, CA), and a fluorometer.

HaCaT cell proliferation assay

HaCaT cells were seeded into 96-well plates at a concentration of 5×10^4 cells per mL in DMEM and incubated for 24 h. For the proliferation assay, HA-EGF conjugates in serum-free media (SFM) were added to HaCaT cells. The serially diluted HA-EGF conjugates in SFM were incubated at 37 °C for 3 days. After 3 days, cell proliferation was assessed by MTT. In control groups, the added amount of EGF or HA/EGF mixture was the same as that of HA-EGF conjugates.

Quantification of VEGF secreted from HaCaT cells

To assess the amount of VEGF secreted from HaCaT cells in response to HA-EGF conjugates, HaCaT cells were seeded into 96-well plates at a concentration of 5×10^4 cells per mL in DMEM and incubated for 24 h. After that, HA-EGF conjugates in SFM were added to HaCaT cells. The serially diluted HA-EGF conjugates in SFM were incubated at 37 °C for 3 days. After 3 days, cell supernatants were sampled and assessed by human VEGF ELISA. The amounts of secreted VEGF were normalized by cell numbers. In control groups, the added amount of EGF was the same as that of HA-EGF conjugates.

***In vitro* scratch assay using HaCaT cells**

The biological activity of EGF or HA-EGF conjugates on HaCaT cells was investigated by the scratch assay. HaCaT cells were seeded into the cell culture plate. After the cells reached 95% confluency, the cells were scraped in a straight line to create a scratch with a p200 pipette tip. Then, the complete medium was replaced with SFM containing EGF or HA-EGF conjugates with the same concentration of EGF. The plates were incubated at 37 °C in a humidified 5% CO₂ cell culture incubator and the migration of the cells was observed by optical microscopy for 2 days.

In vivo treatment of diabetic wound model rats with HA-EGF conjugates

Diabetes mellitus was induced in rats by intraperitoneal injection of STZ (50 mg kg⁻¹) for 5 consecutive days. The blood glucose level was measured with a glucometer at 4 weeks after the first STZ injection. Rats with a blood glucose level higher than 250 mg dL⁻¹ were considered diabetic. A wound was made using an 8 mm biopsy punch at the center of the dorsal skin of each diabetic rat. The rats were randomly divided into four groups (four rats per group) and each wound was topically treated with HA (non-incorporated patch), EGF (EGF-incorporated patch), or HA-EGF conjugates (HA-EGF conjugate-incorporated patch) daily for 16 days. The dose of administered EGF was 1 µg per patch for both EGF and HA-EGF conjugates. The degree of wound healing on the dorsal skin was assessed by measuring the wound area using a digital camera on days 0, 4, 8, 12, and 16. The rate of wound healing was expressed as the percentage of the remaining wound area. The rats were sacrificed 16 days post-treatment for histological analysis and cytokine analysis of wounds. The harvested wound tissues were fixed in 4% formaldehyde at room temperature overnight. The fixed wound tissues were embedded in paraffin, which were cut into serial sections, heated in a vacuum oven at 60 °C for 20 min, deparaffinized, and hydrated. Then, the sections were stained with hematoxylin and eosin (H&E) and Masson's trichrome for standard evaluation and observation of collagen formation in the wound area, respectively. Furthermore, the homogenate of dissected wound tissues was added to the well of an ELISA kit containing 0.1 mL of the lysis buffer, and the cytokine level of the wound tissues was measured by ELISA. To

quantify the amount of collagen in the wound area, the hydroxyproline assay was conducted according to the manufacturer's instructions.

Statistical analysis

Data are expressed as mean ± standard deviation from several separate experiments. Statistical analysis was conducted *via* the unpaired *t*-test for the comparison of the two groups, and the one-way analysis of variance (ANOVA) followed by Dunnett's multiple comparison test was performed for the comparison of more than two groups. The values for **P* < 0.05, ***P* < 0.01, ****P* < 0.001, and *****P* < 0.0001 were considered statistically significant.

Results and discussion

Synthesis and characterization of HA-EGF conjugates

As shown in Fig. 1, we developed an HA patch incorporating HA-EGF conjugates for the treatment of chronic wound healing. After topical application, the HA patch can deliver HA-EGF conjugates in a sustained manner. HA-EGF conjugates can protect EGF from proteolytic degradation by steric hindrance and shielding of HA, interact with the cells in skin tissues such as keratinocytes and fibroblasts *via* receptors of HA and EGF, and stimulate various cell functions for skin tissue regeneration.

We developed three types of HA-EGF conjugates with a MW of 10, 100, or 200 kDa before selecting a suitable HA-EGF conjugate for chronic wound healing. Aldehyde groups were intro-

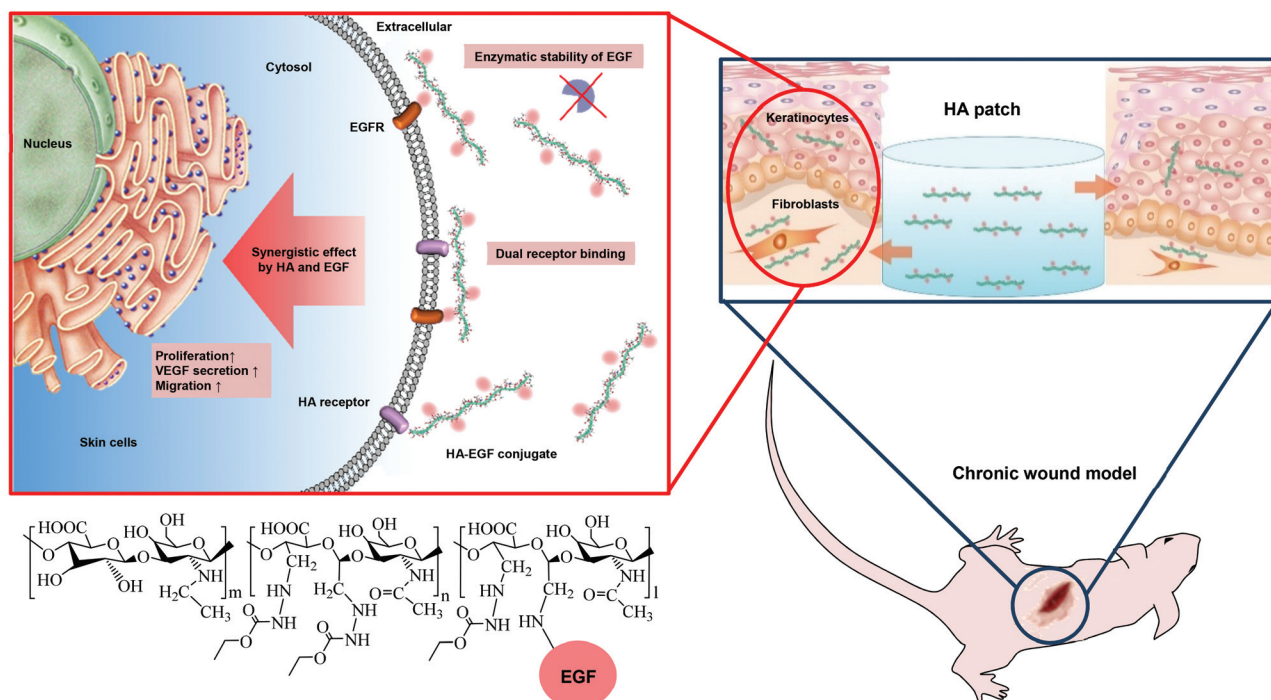


Fig. 1 Schematic illustration of a film type HA patch incorporating HA-EGF conjugates for chronic wound healing.

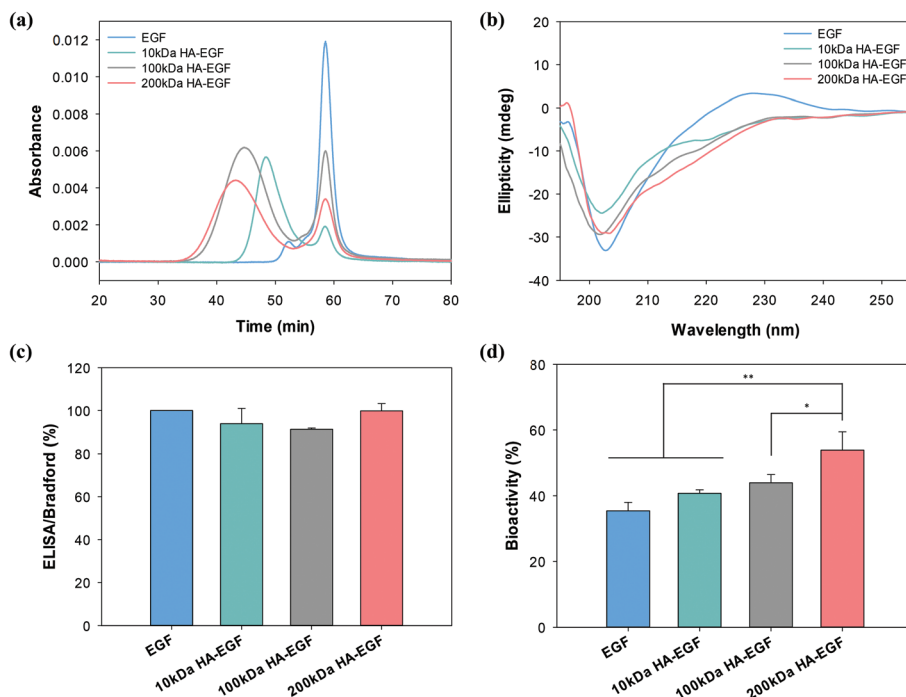


Fig. 2 (a) GPC analysis of EGF and HA-EGF conjugates. (b) CD spectra of EGF and HA-EGF conjugates. (c) The ratios of EGF concentrations in HA-EGF conjugates determined by ELISA and Bradford assay ($n = 3$). (d) The proteolytic degradation of EGF and HA-EGF conjugates 3 h after treatment with trypsin. The trypsin-untreated group is represented as 100% ($n = 3$).

duced into HA molecules by treatment with sodium periodate. Then, EGF molecules were evenly grafted to the aldehyde groups on the long chain of HA by reductive amination. As previously reported elsewhere,¹⁷ during the reaction, aldehyde groups can preferably react with N-terminal primary amine groups of EGF rather than ϵ -amino groups of lysine at a low pH around 5.5 due to the pK_a difference between N-terminal primary amines and lysine amines in EGF. The selective conjugation on N-terminal amine groups can contribute to the maintenance of the secondary structure and biological activity of EGF after conjugation.¹⁷ The successful synthesis of HA-EGF conjugates was confirmed by GPC. As shown in Fig. 2a, the peaks of the three types of conjugates appeared at a shorter retention time than that of EGF. In addition, HA-EGF conjugates with the higher MW of HA showed the shorter retention time. According to the peak area of unreacted EGF before purification, the conjugation efficiency was calculated to be higher than 70%.

The CD analysis revealed that the secondary structure of EGF in HA-EGF conjugates remained stable without significant denaturation, showing a deep negative peak of EGF in the wavelength range of 200–205 nm (Fig. 2b). The immunological bioactivity of HA-EGF conjugates by human EGF ELISA and Bradford assay was comparable to that of native EGF without conjugation (Fig. 2c), likely due to the selective conjugation onto N-terminal amine groups. We also showed that the exposure of EGF to trypsin led to a reduction in EGF activity by ELISA (Fig. 2d). In contrast, HA-EGF conjugates showed high

bioactivity even after treatment with trypsin, confirming the shielding effect of HA from proteolytic degradation. Furthermore, enzymatic stability of HA-EGF conjugates increased with the increasing MW of HA. The enzymatic stability to proteolysis is one of the key factors for *in vivo* improved bioactivity of polymer-conjugated proteins.^{6,8,11,13}

Preparation and characterization of HA patch incorporating HA-EGF conjugates

A recent study showed that the conjugation of the antibody to high MW HA resulted in slow diffusion by six times in the wound bed compared with that of the unconjugated antibody.¹⁸ In the same manner, HA-EGF conjugates may diffuse more slowly than EGF in the wound area. We prepared a film type HA patch incorporating HA-EGF conjugates for more stable and sustained delivery, and convenient operation *in vivo*. The HA patch containing EGF or HA-EGF conjugates for wound healing was prepared by the solvent casting of HA and EGF or HA-EGF conjugate solutions after filling the mixtures into the holes of PDMS molds (Fig. 3a). The patch containing HA-EGF conjugates became a viscous liquid on the wet wound tissue and delivered HA-EGF conjugates in a sustained manner by infiltrating into the wound tissue.

As shown in Fig. 3b, the *in vitro* release profile of HA-EGF conjugates incorporated into the HA patch depending on the MW of HA in the patch matrix. The higher MW of the HA patch showed the slower release of HA-EGF conjugates from the patch. The result might be attributed to the pore

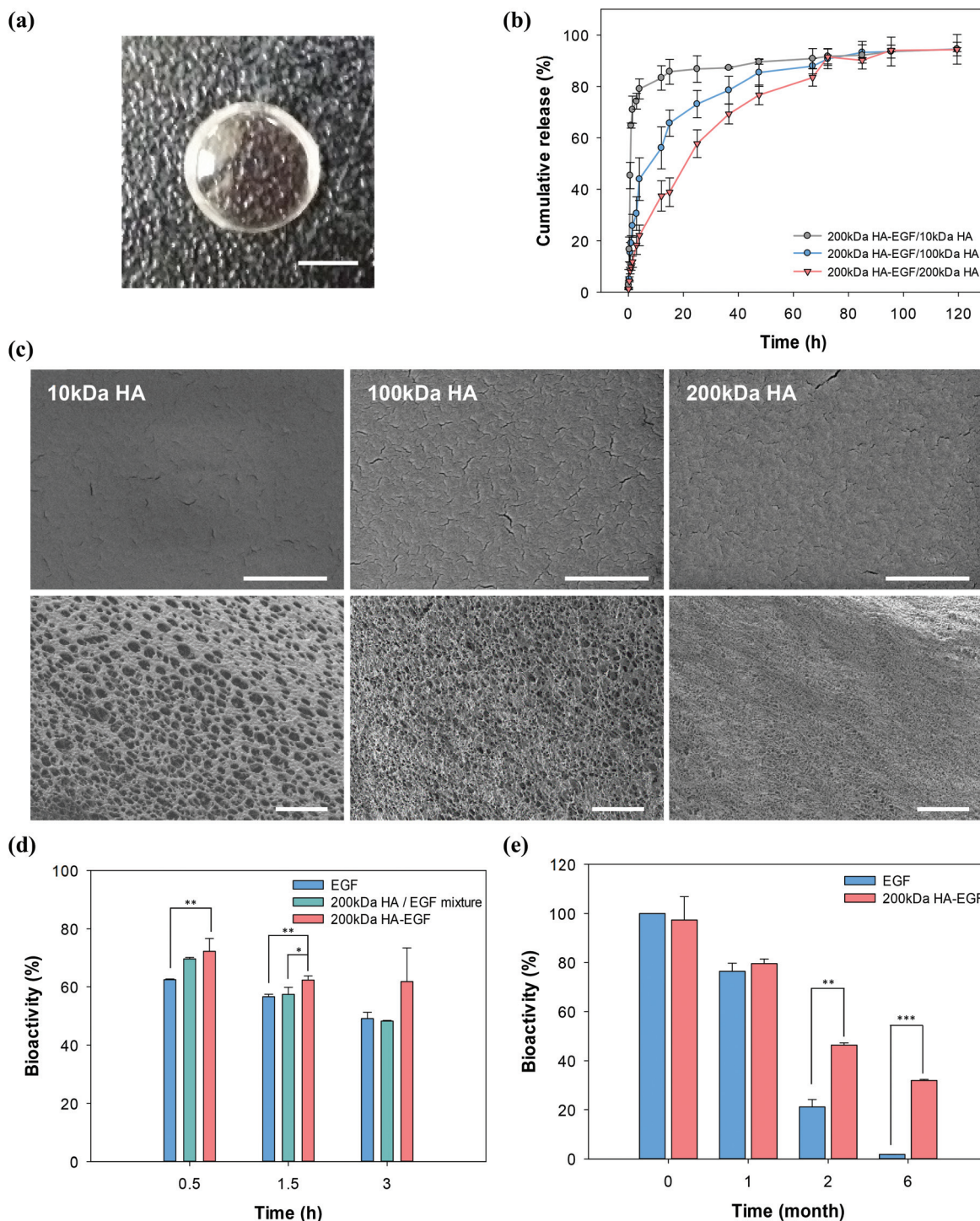


Fig. 3 (a) Photographic image of the HA patch incorporating HA–EGF conjugates (scale bar = 5 mm). (b) *In vitro* release profiles of the HA–EGF conjugate from HA patches ($n = 4$). (c) SEM images of the surface of the HA patch before (top row, scale bar = 1 μm) and after (bottom row, scale bar = 100 μm) hydration. (d) The proteolytic degradation of EGF, HA/EGF mixture, and HA–EGF conjugate by trypsin. The trypsin-untreated group is represented as 100% ($n = 3$). (e) The stability of EGF and HA–EGF conjugates in PBS (pH 7.4) ($n = 3$).

size produced within the HA patch during hydration (Fig. 3c). Before hydration, there was no pore on the surface of the HA patch. After hydration, pores were formed on the surface of the HA patch with the following sizes: 20, 5, and

1 μm in 10, 100, and 200 kDa HA patches, respectively. Since a higher MW HA patch appeared to have smaller pores, incorporated HA–EGF conjugates were likely to be released more slowly.

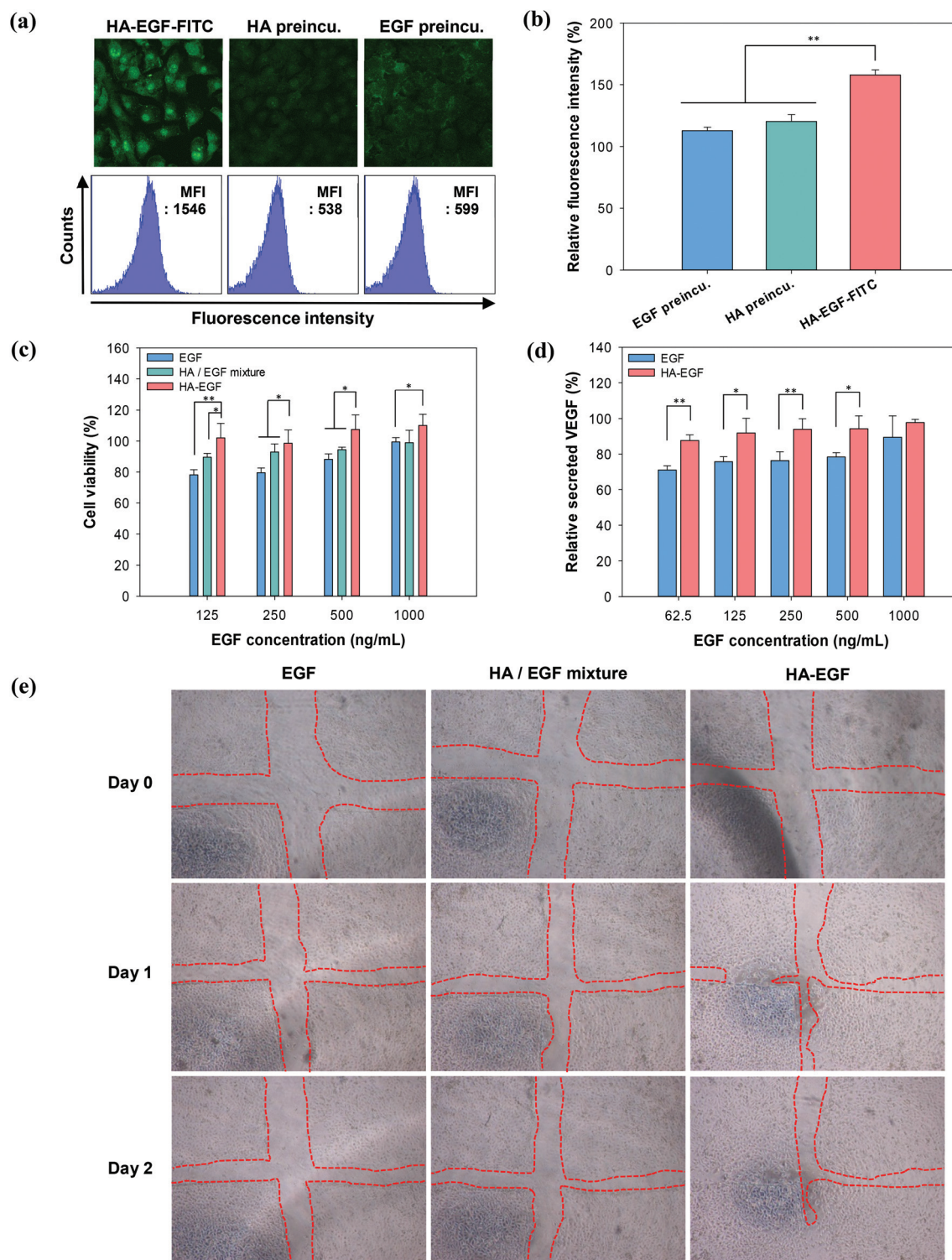


Fig. 4 Effect of 200 kDa HA-EGF conjugate on HaCaT cells. (a) Confocal microscopy images and flow cytometric analysis for the binding of the HA-EGF conjugate to the cells after HA or EGF preincubation ($n = 3$). (b) Quantification of the fluorescence in (a). The non-treated cell group is represented as 100% ($n = 3$). (c) The effect of the HA-EGF conjugate on the cell proliferation with increasing concentration of EGF in serum-free medium. The cultured cell group in complete cell culture medium is represented as 100% ($n = 3$). (d) The effect of the HA-EGF conjugate on the VEGF secretion from the cells treated with HA-EGF conjugate or EGF in serum-free medium. The cultured cell group in complete cell culture medium is represented as 100% ($n = 3$). (e) Optical microscopy images for cell migration after adding EGF, HA/EGF mixture, or HA-EGF conjugate. The red lines represent the boundary between empty region and cells.

To investigate the effect of HA conjugation on EGF stability, we incubated native EGF and HA-EGF conjugates in trypsin (Fig. 3d) and PBS (pH 7.4) solutions (Fig. 3e) for a specified time period. HA-EGF conjugates exhibited superior stability to native EGF, indicating that the conjugation of EGF with a long-chain HA polymer contributed to the protection of the EGF molecule. In addition, the patch-type delivery vehicle in wound healing might protect EGF from degradation and enable a sustained release of sufficient concentrations of active HA-EGF conjugates, resulting in the long-term retention of EGF in the epidermis and dermis.

Effect of HA-EGF conjugates on HaCaT cells

The proliferation and migration of keratinocytes at the wound margin area might contribute to the re-epithelialization process for wound repair. Accordingly, we investigated the effect of the HA-EGF conjugate on the re-epithelialization using HaCaT cells as model keratinocytes. The binding behavior of the HA-EGF conjugate onto HaCaT cells was firstly studied using fluorescence-based methods such as confocal microscopy, flow cytometry, and microplate fluorometric assay. As shown in Fig. 4a and b, the HA-EGF conjugate appeared to bind onto HaCaT cells through both HA-CD44 and EGF-EGFR interactions, reflecting the higher binding affinity of the HA-EGF conjugate than native EGF to HaCaT cells. We further assessed the proliferation and VEGF secretion of HaCaT cells in response to the HA-EGF conjugate. The viability of HaCaT cells treated with the HA-EGF conjugate was higher than that with EGF or HA/EGF mixture at various concentrations of EGF (Fig. 4c). In addition, the amount of VEGF secreted from HaCaT cells in response to the HA-EGF conjugate was also higher than native EGF, indicating that the HA-EGF conjugate might influence the angiogenic process by signaling keratinocytes in the wound bed (Fig. 4d).

The wound closure by the migration of keratinocytes from the surrounding epidermis might also be of pivotal importance. The scratch wound assay revealed that HaCaT cell migration was enhanced in response to the HA-EGF conjugate compared with native EGF (Fig. 4e). As previously reported elsewhere, HA can actively participate in keratinocyte migration and proliferation through interactions with the HA receptors of CD44 and RHAMM.¹⁹ From this point of view, the HA/EGF mixture might induce a higher migration and proliferation effect than native EGF through the synergistic effect of HA and EGF. Remarkably, the migratory and proliferative capacities of the HA-EGF conjugate were superior to those of the HA/EGF mixture. The result might be explained by the multivalent binding affinity of the HA-EGF conjugate on HaCaT cells *via* the synergistic effect of HA and EGF.^{20,21} In a similar study, multivalent conjugation of the growth factor Sonic hedgehog (Shh) to HA yielded enhanced Shh-pathway activation, inducing the angiogenic function compared with that by the equivalent dose of unconjugated Shh.²²⁻²⁴ Although the underlying signaling mechanism caused by the HA-EGF conjugate requires further investigation, the HA-EGF conjugate can certainly increase keratinocyte proliferation, VEGF secretion, and migration, likely contributing to the fast re-epithelialization during wound repair.

In vivo assessment of HA-EGF conjugate incorporated into the HA patch

Diabetes was induced into rats by intraperitoneal daily injection (50 mg kg⁻¹) of STZ for 5 days. The blood glucose level was measured at 4 weeks after the first STZ injection using a glucometer. Rats with a blood glucose level higher than 250 mg dL⁻¹ were considered diabetic. The chronic wound model was induced using an 8 mm biopsy punch at the center of the dorsal skin of each diabetic rat and the wound healing

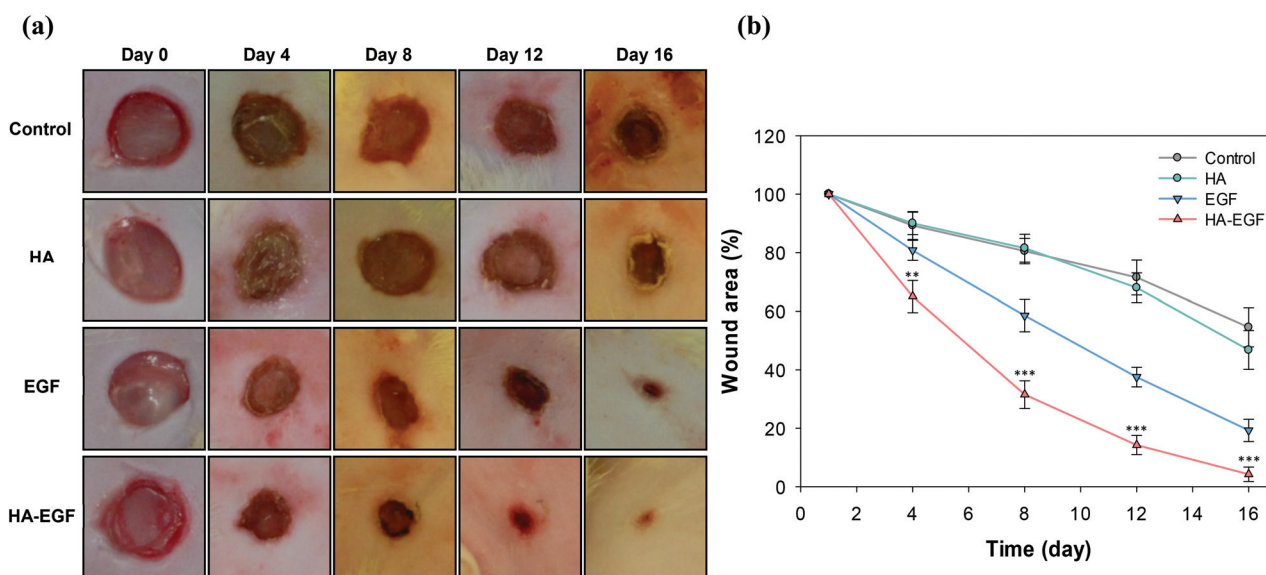


Fig. 5 (a) Photographic images of wound areas for 16 days and (b) changes in the measured area after treatment of 200 kDa HA patches with incorporated EGF or 200 kDa HA-EGF conjugate ($n = 4$). ** $P < 0.01$ and *** $P < 0.001$ versus EGF-treated group.

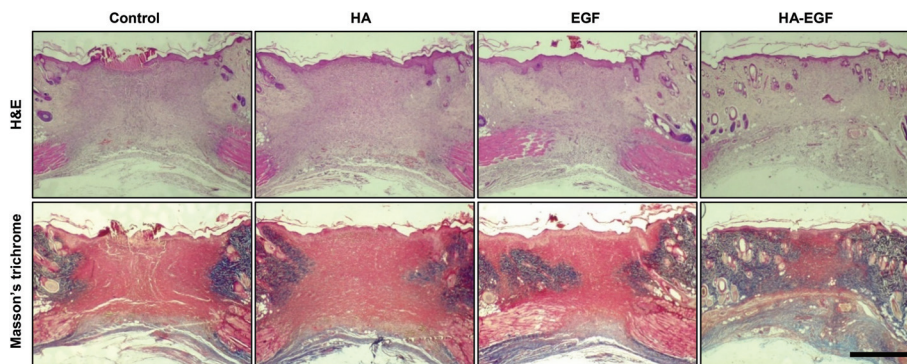


Fig. 6 Histological analysis with H&E staining and Masson's trichrome staining 16 days after treatment with 200 kDa HA patch with incorporated EGF or 200 kDa HA-EGF conjugate on diabetic wound model tissues (scale bar = 500 μm).

process was evaluated after treatment with HA-EGF conjugates incorporated into the HA patch. After wound formation, the wound area is hydrated within 5–10 min by the wound fluid effused from the scar. The HA patch appeared to be swollen and slowly dissolved into the viscous liquid. The dissolved HA patch could be steadily attached to the wound area. As shown in Fig. 3b, the HA-EGF conjugate might diffuse from the viscous gel-like solution. To measure the wound size, the wound area was photographed every 4 days (Fig. 5a). The wound area measured each day was normalized by considering the initial wound area as 100% (Fig. 5b). The half healing time (HT_{50}), which is the time required for the reduction of the wound area to half of its initial size, was calculated by extra-

polating from the measured data. Although the wound size decreased by natural healing for the untreated control group, the wound closure was accelerated for groups treated with EGF and HA-EGF conjugate incorporated into the HA patch. The HT_{50} for the HA-EGF conjugate was only 5.8 days, which was much lower than 9.5 days for the EGF group, reflecting the healing effect of HA-EGF conjugates on the skin wound.

Histological analysis with H&E staining and Masson's trichrome staining was performed for further therapeutic analysis (Fig. 6). On the punched skin tissues, damaged skin tissues showed loosely arranged and less granulated tissue structures. However, after treatment with the HA-EGF conjugate incorporated into the HA patch, the damaged area was

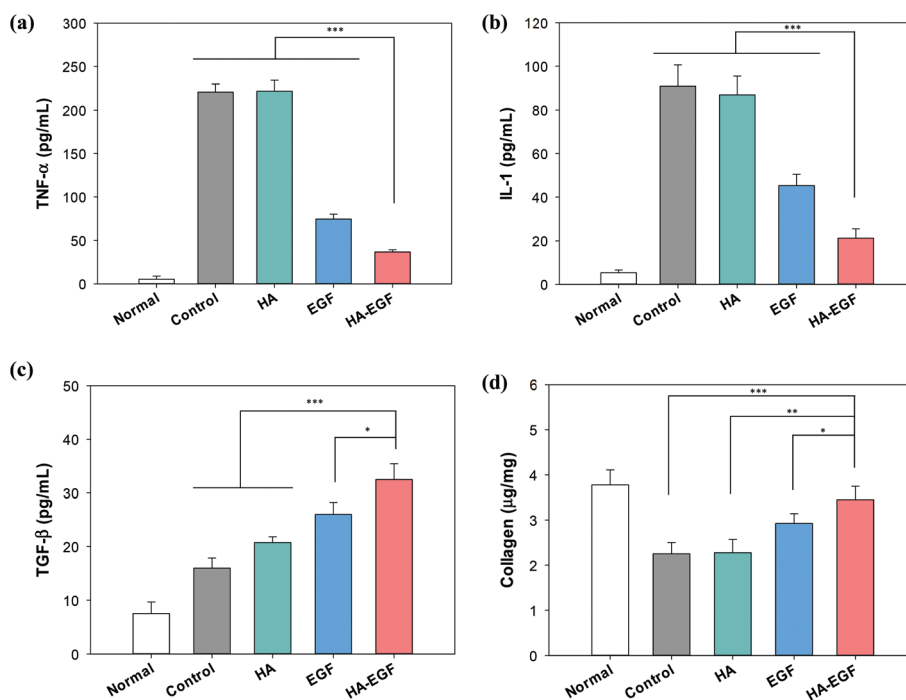


Fig. 7 Cytokine analysis of (a) TNF- α , (b) IL-1 and (c) TGF- β and hydroxyproline assay of (d) collagen content in the homogenate of the dissected wound tissues 16 days after treatment with 200 kDa HA patches with incorporated EGF or 200 kDa HA-EGF conjugate on diabetic wound model ($n = 4$).

significantly reduced and the border between damaged and normal tissues was ambiguous compared with other groups. In addition, the recovered skin tissues showed almost complete re-epithelialization and granulation of dermal tissues. Particularly, the HA-EGF conjugate-treated group showed a mostly recovered hypodermis structure with white granular tissues, which might be attributed to the biological interaction of HA-EGF conjugates with skin cells and the prolonged residence of the HA-EGF conjugate. In consistent with the results of H&E staining, Masson's trichrome staining also showed the positive effect of the HA-EGF conjugate on skin wound healing. The remarkable collagen deposition in the dermis of the regenerated skin was observed at day 16 with the strongest blue staining intensity for the regenerated collagens.

The cytokine analysis in skin tissues also supported the therapeutic effect of the HA-EGF conjugate incorporated into the HA patch (Fig. 7a-c). The HA-EGF conjugate reduced the high level of inflammatory cytokines such as TNF- α and IL-1 more effectively than other groups including the EGF-treated group. The HA-EGF conjugate incorporated into the HA patch also significantly elevated the level of TGF- β known to stimulate cellular proliferation. The collagen content in wound tissues was also drastically enhanced after treatment with the HA-EGF conjugate at day 16, as shown in Fig. 7d. All these results revealed the therapeutic effect of the patch-type HA-EGF conjugates on skin wound healing by the prolonged residence of EGF in wound tissues, the long-term release of the conjugate from the HA patch, and the improved interaction with skin cells. Similarly, recent other studies have demonstrated that HA conjugation could increase the activity of proteins.^{18,22-27} The cytokine neutralizing HA-antibody conjugates appeared to strengthen the binding affinity for inflammation mediators with the simultaneous activation of CD44/RHAMM and the suppression of cytokine-signaling networks.²⁵ The used HA with a MW of 100-300 kDa was also reported to promote wound healing.²⁸ In addition, as previously reported elsewhere,^{14,29} the HA-EGF conjugate might be delivered efficiently into deep skin tissues. Taken together, the HA-EGF conjugate might be successfully developed for the treatment of chronic wounds with advantages such as facilitating topical delivery and interaction with dual receptors, and alleviating the degradation of EGF in diabetic chronic wounds.

Conclusions

We developed a HA-EGF conjugate incorporated into a HA patch for diabetic wound healing. HA-EGF conjugates were synthesized by conjugating the amine group of EGF to aldehyde-modified HA by reductive amination. After *in vitro* characterization for improved enzymatic stability and biological activity of HA-EGF conjugates on skin cells, we incorporated HA-EGF conjugates into the HA patch by a simple drying method at room temperature for sustained long-term delivery to the skin wound. The HA-EGF conjugate incorporated into the HA patch showed a more significant *in vivo* wound healing

effect than the other control samples including EGF. The conjugation of HA with EGF appeared to protect EGF against enzyme degradation and enhance proliferation, VEGF secretion, and migration of human keratinocytes through both HA-CD44 and EGF-EGFR interactions. From all these results, we could confirm the feasibility of the HA-EGF conjugate patch for diabetic wound healing applications.

Conflicts of interest

There are no conflicts to declare.

Acknowledgements

This research was supported by the Nano-Material Technology Development Program (No. 2017M3A7B8065278) and the Basic Science Research Program (2017R1E1A1A03070458) of the National Research Foundation (NRF) funded by the Ministry of Science, ICT & Future Planning, Korea. This work was also supported by the World Class 300 Project (R&D) (S2482887) of the Small and Medium Business Administration (SMBA), Korea.

References

- 1 D. Chouhan, B. Chakraborty, S. K. Nandi and B. B. Mandal, *Acta Biomater.*, 2017, **48**, 157-174.
- 2 G. S. Schultz, R. G. Sibbald, V. Falanga, E. A. Ayello, C. Dowsett, K. Harding, M. Romanelli, M. C. Stacey, L. Teot and W. Vanscheidt, *Wound Repair Regen.*, 2003, **11**, 1-28.
- 3 R. B. Greenwald, Y. H. Choe, J. McGuire and C. D. Conover, *Adv. Drug Delivery Rev.*, 2003, **55**, 217-250.
- 4 E. M. Pelegri-O'Day, E. W. Lin and H. D. Maynard, *J. Am. Chem. Soc.*, 2014, **136**, 14323-14332.
- 5 A. J. Keefe and S. Jiang, *Nat. Chem.*, 2012, **4**, 59-63.
- 6 J. Hardwicke, E. L. Ferguson, R. Moseley, P. Stephens, D. W. Thomas and R. Duncan, *J. Controlled Release*, 2008, **130**, 275-283.
- 7 J. Hardwicke, R. Moseley, P. Stephens, K. Harding, R. Duncan and D. W. Thomas, *Mol. Pharmaceutics*, 2010, **7**, 699-707.
- 8 J. T. Hardwicke, J. Hart, A. Bell, R. Duncan, D. W. Thomas and R. Moseley, *J. Controlled Release*, 2011, **152**, 411-417.
- 9 R. O. Hynes, *Science*, 2009, **326**, 1216-1219.
- 10 H. Chu, N. R. Johnson, N. S. Mason and Y. Wang, *J. Controlled Release*, 2011, **150**, 157-163.
- 11 S. J. Paluck, T. H. Nguyen, J. P. Lee and H. D. Maynard, *Biomacromolecules*, 2016, **17**, 3386-3395.
- 12 T. H. Nguyen, S. J. Paluck, A. J. McGahran and H. D. Maynard, *Biomacromolecules*, 2015, **16**, 2684-2692.
- 13 T. H. Nguyen, S. H. Kim, C. G. Decker, D. Y. Wong, J. A. Loo and H. D. Maynard, *Nat. Chem.*, 2013, **5**, 221-227.
- 14 J. A. Yang, E. S. Kim, J. H. Kwon, H. Kim, J. H. Shin, S. H. Yun, K. Y. Choi and S. K. Hahn, *Biomaterials*, 2012, **33**, 5947-5954.

- 15 K. L. Aya and R. Stern, *Wound Repair Regen.*, 2014, **22**, 579–593.
- 16 G. Gainza, D. C. Bonafonte, B. Moreno, J. J. Aguirre, F. B. Gutierrez, S. Villullas, J. L. Pedraz, M. Igartua and R. M. Hernandez, *J. Controlled Release*, 2015, **197**, 41–47.
- 17 H. Lee, I. H. Jang, S. H. Ryu and T. G. Park, *Pharm. Res.*, 2003, **20**, 818–825.
- 18 E. E. Friedrich and N. R. Washburn, *Biomaterials*, 2017, **114**, 10–22.
- 19 Y. Xie, Z. Upton, S. Richards, S. C. Rizzi and D. I. Leavesley, *J. Controlled Release*, 2011, **153**, 225–232.
- 20 R. S. Kane, *Langmuir*, 2010, **26**, 8636–8640.
- 21 R. H. Kramer and J. W. Karpen, *Nature*, 1998, **395**, 710–713.
- 22 S. T. Wall, K. Saha, R. S. Ashton, K. R. Kam, D. V. Schaffer and K. E. Healy, *Bioconjugate Chem.*, 2008, **19**, 806–812.
- 23 T. Vazin, R. S. Ashton, A. Conway, N. A. Rode, S. M. Lee, V. Bravo, K. E. Healy, R. S. Kane and D. V. Schaffer, *Biomaterials*, 2014, **35**, 941–948.
- 24 B. W. Han, H. Layman, N. A. Rode, A. Conway, D. V. Schaffer, N. J. Boudreau, W. M. Jackson and K. E. Healy, *Tissue Eng., Part A*, 2015, **21**, 2366–2378.
- 25 L. T. Sun, S. A. Bencherif, T. W. Gilbert, A. M. Farkas, M. T. Lotze and N. R. Washburn, *Wound Repair Regen.*, 2010, **18**, 302–310.
- 26 T. A. Holstlaw, M. Mahomed, L. W. Brier, D. M. Young, N. J. Boudreau and W. M. Jackson, *Biomacromolecules*, 2017, **18**, 2350–2359.
- 27 E. I. Altiok, J. L. Santiago-Ortiz, F. L. Svedlund, A. Zbinden, A. K. Jha, D. Bhatnagar, P. Loskill, W. M. Jackson, D. V. Schaffer and K. E. Healy, *Biomaterials*, 2016, **93**, 95–105.
- 28 K. Ghazi, U. Deng-Pichon, J. M. Warnet and P. Rat, *PLoS One*, 2012, **7**, e48351.
- 29 J. K. Choi, J.-H. Jang, W.-H. Jang, J. Kim, I.-H. Bae, J. Bae, Y.-H. Park, B. J. Kim, K.-M. Lim and J. W. Park, *Biomaterials*, 2012, **33**, 8579–8590.